Journal of the European Ceramic Society **19** (1999) 207–215

PII: S0955-2219(98)00185-X
0955-2219/98/$—see front matter

Fatigue Damage Accumulation in 3-Dimensional SiC/SiC Composites

V. Kostopoulos,* Y. Z. Pappas and Y. P. Markopoulos

Applied Mechanics Laboratory, University of Patras, Patras University Campus, 265 00 Patras, Greece

(Received 18 February 1998; revised version received 9 July 1998; accepted 31 July 1998)

Abstract

The effect of fatigue loading on the mechanical performance of 3-D SiC/SiC composites was investigated. A non-destructive macromechanical approach was applied which permits for the evaluation of the material damage state by monitoring its dynamic response as function of fatigue cycles. The correlation of the results provided by this method to that of other non-destructive techniques such as Acoustic Emission (AE), leads to a detail micromechanical-macromechanical monitoring of the material fatigue behaviour. The damage modes identification and their successive appearance, together with the evaluation of the material performance at the different stages of fatigue loading, is among the inspection capabilities that provides the above mentioned combination of non-destructive techniques. The proposed methodology applied in the case of a 3-D SiC/SiC ceramic matrix composite material and the effect of fatigue loading on the material integrity was evaluated by measuring the degradation of the dynamic modulus of elasticity and the increase of the material damping. Conclusions, concerning design aspects using these materials, as well as fatigue life prediction were provided. Finally, the sensitivity of the proposed methodology for the definition, the characterisation of the development and the separation of the different damage modes during fatigue loading has been discussed. © *1998 Elsevier Science Limited. All rights reserved*

Keywords: composites, fatigue, SiC, failure analysis: acoustic emission.

1 Introduction

It is well known that subcritical fatigue loading of composite structures is responsible for the development of damage modes, which affects the performance and the life of the structure. The damage propagation, the interaction between the different damage modes and the resulting damage accumulation promotes critical damage modes within the composite structure, alters the material stiffness and damping characteristics and reduces the strength together with the fatigue life of the composite laminates.

More precisely, subcritical fatigue loading of ceramic matrix composites (CMCs) appears whenever the maximum applied cyclic stress exceeds the matrix strength for cracking. Then, the cyclic opening and closing of matrix cracks is the basic responsible mechanism of fatigue for CMCs.[1]

During fatigue, the fibre–matrix interfaces debond and slide between fibre and matrix is established as matrix cracking extends. Macroscopically, the damage development during fatigue in CMCs manifests itself by the appearance of stress-strain hysterisis loops, which are more wide increasing the fatigue cycles (whenever the matrix cracking is not saturated[2]), the presence of inelastic-permanent strain, the decrease of the modulus of elasticity and the decrease of the tensile strength of the material. Each time, the intensity of the above described effects is strongly related to the material system under consideration, the type of the reinforcement structure and finally the residual stress field that experiences the given CMC system.

During the last years, some work has been done to the direction of understanding and quantifying the fatigue effect on ceramic matrix composites.[3–9] Among them, the pioneer work of Kotil *et al.*[4] who first tried to model the hysterisis loops appeared during the fatigue of UD CMCs and the very informative overview of Evans *et al.*[1] where the role of the fibre and the matrix material has been discussed analytically for both 1-D and 2-D reinforcement architecture, the cyclic crack growth has been quantified and a methodology for

*To whom correspondence should be addressed. E-mail: kostopoulos@tech.mech.upatras.gr

the fatigue life prediction has been proposed. In all the cases it is always emphasised:

- The critical role of fibre–matrix interface, its degradation during fatigue and the development of a sliding stress which diminishes upon cycling.
- The presence of the hysterisis loops which show that inelastic strain increases, elastic modulus decreases together with a loop widening as fatigue proceeds and the matrix cracking has not reached the saturation point.

In the present work the problem of fatigue behaviour of CMCs has been treated through a macroscopical approach, where both the stiffness degradation and the hysterisis loop widening during fatigue were monitored indirectly using the change in the dynamic response of the fatigued components, i.e. by measuring the eigenfrequency spectrum and the corresponding modal damping characteristics. Then, assuming an apparent linear viscoelastic behaviour for the material under consideration, the eigenfrequency and the modal damping measurements were transformed to material properties (stiffness and loss factor).

The evaluation of the fatigue effect through the variation of the apparent viscoelastic properties of the material system under testing has been applied first in the case of organic matrix composites[10,11] and the loss factor has been identified as a very useful parameter for fatigue life prediction since it is much more sensitive to fatigue compared to the stiffness.

Within the frame of this study, the effect of the fatigue loading of 3-D SiC/SiC composite on both the dynamic modulus of elasticity and the damping coefficient (loss factor) were investigated. According to the obtained results, modal damping measurements or equivalently loss factor calculations could be a reliable measure of the fatigue damage state in the case of CMCs. This was expected, since modal damping is a measure of the energy loss per cycle of vibration and it is in a direct relation to the area of the hysterisis loop at a given fatigue cycle. What makes the modal damping more attractive as a descriptor for the evaluation of the fatigue damage state in CMCs is the easy way of measuring it under real working conditions.

Furthermore, in order to correlate the macroscopical monitored fatigue damage state to the microscopical failure mechanisms, which are responsible for the material deterioration, continuous acoustic emission monitoring has been performed during fatigue. Acoustic emission data have been corresponded to the main failure mechanisms and the activation of these mechanisms have been correlated to the changes in the dynamic response of 3-D SiC/SiC composite. Finally, the use of modal damping as a descriptor for the fatigue life prediction in the case of CMCs has been discussed analytically.

2 Experimental Procedure

2.1 Description of the material

The 3-dimensional (3-D) SiC/SiC material was produced by Aerospatiale Bordeaux as a part of a Brite/Euram Project entitled 'Development and Characterization of CMC and C/C Composites' (Contract No. BREU 0334-C). The 3-D SiC/SiC material was made out of Nicalon fibres and a metal-organic based Silicon Carbide matrix. The woven fibre perform has a 3-dimensional orthogonal architecture shown in Fig. 1. The development of the material includes optimisation of all the seven basic manufacturing steps.[7,8] The final product has a density of $2{\cdot}1\,\mathrm{gr\,cm^{-3}}$ and an open porosity of about 20%. The fibre volume fraction is 36%, equally distributed in the three rectangular directions. Plates of 6 mm thickness were manufactured. The mean diameter of the fibre bundles is of the order of 1 mm. The material can be used up to 1200°C, however, an oxidation protection layer is necessary for oxidative application above 500°C.

2.2 Testing procedure

A group of 3-D SiC/SiC straight strip specimens with gauge length 200 mm, width 10 mm and thickness 6 mm (the original plate thickness) were tested, according to ENV 1893 standards for tensile and fatigue tests for advanced ceramics. Tapered aluminium end-tabs were bonded at the gripping area of the specimens using epoxy resin (Ciba LY-564 / hardener HY 2954).

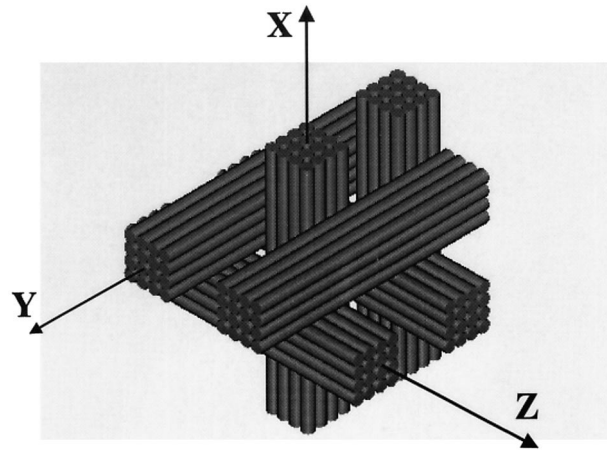

Fig. 1. Schematic representation of the 3-D SiC/SiC orthogonal preform.

Tension–tension fatigue tests were performed under load control condition. The cyclic frequency was 10 Hz having a sinusoidal wave form and the stress ratio was $R = 0{\cdot}1$ ($R = \sigma_{min}/\sigma_{max}$). Tensile tests were also accomplished using a cross head velocity of 0·1 mm/min, in order to have a complete material characterization.

All the test were carried out on a closed loop servo-hydraulic testing machine equipped with a hydraulic gripping system, at room temperature, in air. During both tensile and fatigue tests, acoustic emission (AE) activity was monitored using a 150 kHz resonant transducer and AE events were tracked using a Physical Acoustic Corporation (SPARTAN AT 8000) system. The acoustic emission parameters used were total amplification level 20 dB, threshold 60 dB, peak definition time 30 μs and a high-pass filter of cut-off frequency of 100 kHz.

2.3 Measurements of the dynamic response

The effect of fatigue on both effective dynamic modulus of elasticity and the relative loss factor (damping coefficient) was investigated using the free flexural vibration of test coupons exposed to fatigue. The following procedure was applied.

Initially, each sample before being subjected to fatigue, was tested to free flexural vibration triggered by an initial velocity, under a cantilever beam configuration. The response of the specimen was monitored by an accelerometer having a mass of 0·5 g, which was mounted on the free edge of the specimen. The accelerometer had a dynamic range of 500 g (g = 9·81m s^{-2} and a sensitivity of 3·46 mV g^{-1}.

In the sequence, the specimen was loaded to tension–tension fatigue up to fracture or up to a number of fatigue cycles defined as endurance fatigue limit (10^6 cycles). At regular time intervals corresponding to 10, 20, 50, 100, 200,...,1000 kcycles, the fatigue process was stopped, the upper part of the gripping system was opened and the accelerometer was mounted again on the free edge of the specimen. Following this procedure both fatigue and boundary conditions for the free flexural vibration experiment were secured unchanged. Then, the specimen was exposed again to free flexural vibration and its response was monitored. An A/D board (National Instrument 2000) with 2·5 mV sensitivity and maximum sampling frequency 1 MHz, connected to a PC was used to collect and store the amplified analogue signal of the accelerometer. FFT analysis of the signal of accelerometer provides the eigenfrequency spectrum of the vibrated specimen. Short FFT analysis of the same signal furnishes the decay rate of the amplitude at each mode shape (modal damping) for each specimen. The results are presented in the form of normalised data using reference values the relative results of the same initially tested virgin specimen. A schematic representation of the experimental set up for the monitoring of the dynamic response of the tested samples is given in Fig. 2(a).

Figure 2(b) shows the experimental set up, which was used for AE measurements. The following AE parameters were monitored continuously during the fatigue experiment: Amplitude (A), Rise Time (RT), Energy (E), Duration (D) and Counts (C). Their physical meaning is has been extensively discussed.[12] Applying pattern recognition techniques, which are presented in detail elsewhere,[13] the AE events which correspond to fibre breakage have been separated.

2.4 Theoretical analysis

In the present Section, the inversion algorithm, in order to calculate the dynamic material properties based on the eigenfrequency and modal damping measurements, will be given. The material of the vibrating beam assumed to be macroscopically homogeneous and transversely isotropic exhibits linear viscoelastic behaviour. The latter assumption consists of the theoretical tool for incorporating frequency dependent damping behaviour in the present analysis. The specimen, which experiences the flexural vibration is of rectangular cross section and has been supported under cantilever configuration.

The differential equation which describes the free vibration of a linear viscoelastic beam and fulfils the Euler–Bernoulli assumptions is given by

$$a_c^2 \frac{\partial^4 w^c(x,t)}{\partial x^4} + \frac{\partial^2 w^c(x,t)}{\partial t^2} = 0 \qquad (1)$$

where w^c is the transverse displacement of the beam and a_c^2 a complex constant. The explicit form of a_c^2 is given by the relation

$$a_c^2 = \frac{1}{\rho h \left[D_{xx}^c\right]^{-1}} \qquad (2)$$

where ρ is the linear density of the vibrating beam, h is the thickness of the beam and $\left[D_{xx}^c\right]^{-1}$ is the element of the inverse of the bending stiffness matrix $[D^c]$. D_{xx}^c is account as the complex bending stiffness of the 3 D SiC/SiC along the loading direction according to the analysis presented elsewhere.[14] Assuming harmonic time dependence eqn (1) obtains the form

$$\frac{\partial^4 w^c(x)}{\partial x^4} - \frac{\omega^2}{a_c^2} w^c(x) = 0 \qquad (3)$$

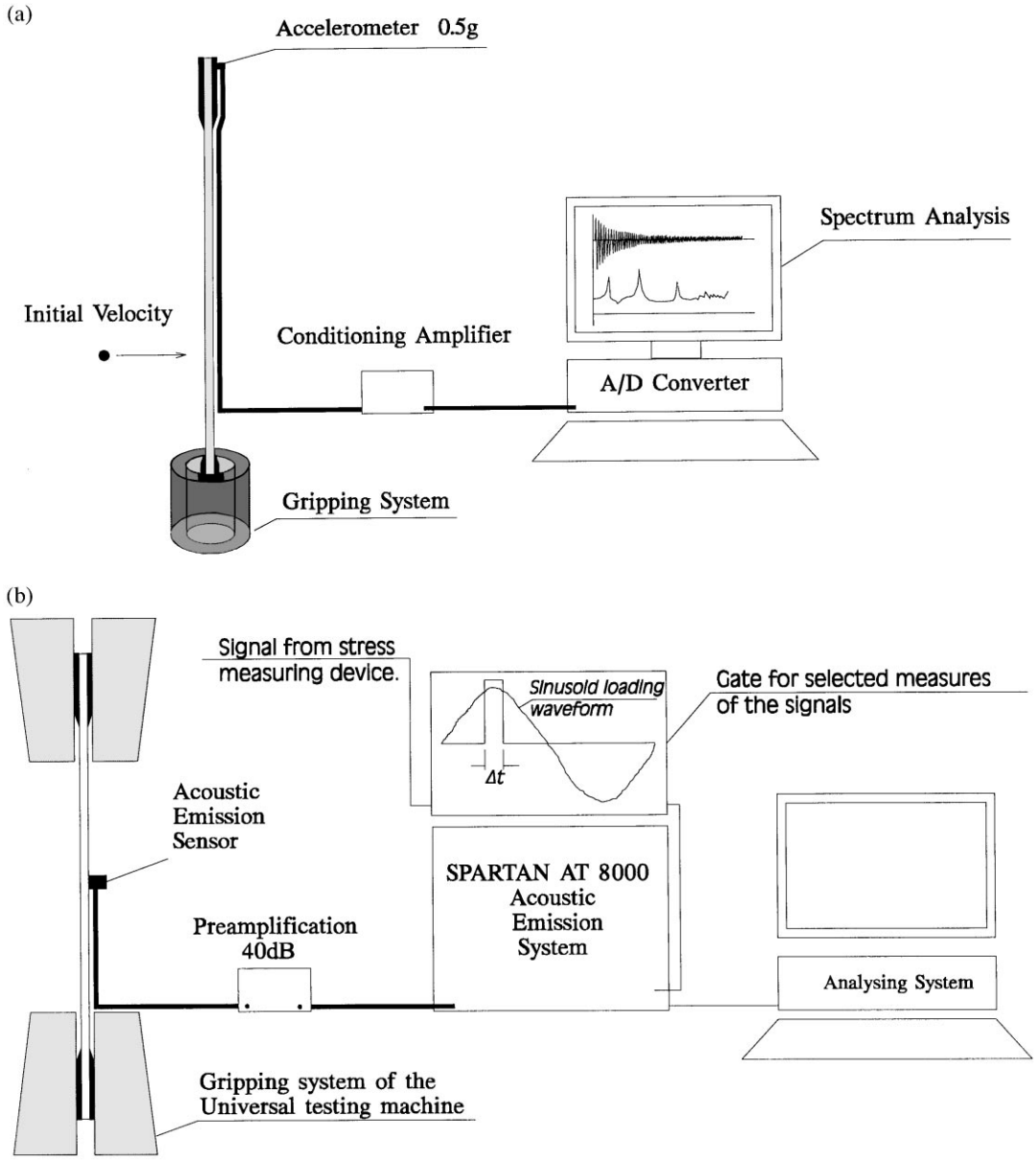

Fig. 2. (a) Representation of the experimental set up for the dynamic response measurements; (b) Representation of the experimental set up for the acoustic emission measurements.

The general solution of eqn (3) exhibits the form

$$W_n(x,t)=\left\{C^c_{1n}e^{\kappa_n x}+C^c_{2n}e^{-\kappa_n x}+C^c_{3n}e^{i\kappa_n x}+C^c_{4n}e^{-i\kappa_n x}\right\} \tag{4}$$

where the following relation has been used

$$k_n^4=\frac{\omega_n^{c_2}}{a_c^2} \tag{5}$$

Assuming the wave number $k\varepsilon\rho$ then the vibration frequency is a complex quantity of the form

$$\omega_n^c=\omega_n-id_n \tag{6}$$

and for physical reasons Imposing for $\left[D^c_{xx}\right]^{-1}$ the form that contains the effective complex bending modulus of elasticity then

$$\begin{aligned}\left[D^c_{xx}\right]^{-1}&=\frac{12}{h^3}\cdot\frac{1}{E^{c,e}_{xx}}=\frac{12}{h^3}\frac{1}{E^{R,e}_{xx}\left(1+n^e_{xx}\right)}\\&=\frac{12}{h^3}\cdot\frac{1}{|E^{c,e}_{xx}|e^{i.\arctan\left[n^e_{xx}\right]}}\end{aligned} \tag{7}$$

where $E^{R,e}_{xx}$ is the real part of $E^{c,e}_{xx}$, $|E^{c,e}_{xx}|$ is the measure of $E^{c,e}_{xx}$ and n^e_{xx} is the effective loss factor which is defined as

$$n^e_{xx}=\frac{E^{I,e}_{xx}}{E^{R,e}_{xx}}\left(E^{I,e}_{xx}\text{ is the imaginary part of }E^{c,e}_{xx}\right) \tag{8}$$

Finally the application of the boundary conditions for the case of a cantilever beam concludes to the following expression for the eigenfrequencies of the problem[14]

$$\omega_n = \sqrt{\frac{k^4h^2}{12\rho}.|E_{xx}^{c,e}|}.\cos\left(\frac{\arctan(n_{xx}^e)}{2}\right) \quad (9)$$

$$d_n = \sqrt{\frac{k^4h^2}{12\rho}.|E_{xx}^{c,e}|}.\sin\left(\frac{\arctan(n_{xx}^e)}{2}\right) \quad (10)$$

and in case of knowing/measuring ω_n and d_n then the unknown quantities are $|E_{xx}^{c,e}|$ and n_{xx}^e. Solving eqns (9) and (10) with respect to $|E_{xx}^{c,e}|$ and n_{xx}^e one obtains[14]

$$|E_{xx}^{c,e}| = \left(\omega_n^2 + d_n^2\right).\frac{12\rho}{k^4h^2} \quad (11)$$

$$n_{xx}^e = \tan\left(2.\arctan\left(\frac{d_n}{\omega_n}\right)\right) \quad (12)$$

Equations (11) and (12), are the expressions which will be applied in the next in order to calculate the effective complex modulus of elasticity.

3 Results and Discussion

The tensile and fatigue properties of 3-D SiC/SiC composites are reported in Table 1.[8] During fatigue, whenever the maximum applied stress exceeds the strength of the matrix material, an extensive matrix crack network is established within the 3-D SiC/SiC structure. This, together with the matrix cracks produced during the processing phase, and the accompanied fibre matrix debonding consist the first obvious group of damage mechanisms, which are developed during the first fatigue cycle. Depending upon the magnitude of the maximum applied stress, the matrix cracking may or may not reach the saturation point, which is denoted by a characteristic spacing of the matrix cracks. Once the maximum applied load exceeds the stress related to the saturation point, then the load is transferred by the fibres and macroscopically the material appears as an almost linear stress–strain curve which deviates from linearity once fibre failures initiate.

Table 1. Tensile and fatigue properties of 3-D SIC/SiC composites

	Mean value	*SDD*
Tensile strength (UTS) (MPa)	161	0·7
Tensile tangent modulus of elasticity (GPa)	27	0·7
Endurance fatigue limit ($R=0{\cdot}1$, $f=10$Hz) (% UTS)	70	0·02

The above given statements mainly concern the development of the damage modes during the first fatigue cycle and their dependence upon the maximum applied fatigue stress. However, summarising the fatigue modes appearing during fatigue tests performed on 3-D SiC/SiC composites the following may be concluded.[7,8]

- Matrix cracking is the first damage mode appearing during the first fatigue cycle, whenever the applied maximum fatigue stress exceeds the strength of the matrix material. Matrix cracking typically stabilises very early in the fatigue life of 3-D SiC/SiC composites.
- The initially developed matrix crack network is combined with the already existed, due to processing, matrix cracks and matrix porosity and under the applied cyclic loading leads to the saturation point for the matrix cracking. During this stage, the matrix cracking is accompanied by an extensive fibre matrix debonding. Once the matrix cracking saturates, the matrix is cracked and the fibres are sufficiently debonded, the stress–strain curve regains an almost linear form.[6]
- Although matrix cracking is prerequisite for fatigue failure, does not control the fatigue life.[6] The extensive matrix cracking and the interfacial debonding result in the interfacial sliding and wear. Additionally, in the vicinity of the intersection points in the case of 3-D SiC/SiC composites, the matrix cracking and the interfacial debonding reduce the stress concentration and allow for a better alignment of the fibre preform to the loading direction. During both phenomena extensive frictional slip is presented.
- Finally, fibre fractures are localised during a short period at the end of the fatigue life, although there are some fibre failures during the first fatigue cycle even when the applied maximum fatigue load does not exceed the endurance fatigue limit.

3.1 Dynamic characterisation of 3-D SiC/SiC composites

In the present case of 3 D SiC/SiC composites, two different groups of fatigue tests were performed and the 'stop and go' procedure described earlier was applied. Using this procedure the monitoring of the variation of the effective dynamic modulus of elasticity along the loading direction of 3-D SiC/SiC composites and the associated loss factor have been provided as a function of the number of fatigue cycles.

The maximum applied stress for the first group was 0·7 of the ultimate tensile strength (UTS) of

3-D SiC/SiC composites, while for the second one it was 0·75 of UTS. Each group was consisted by four samples. The results presented in the next are referred to the monitored mean value of the presented parameter for four specimens in the case of the test specimens loaded up to a maximum applied load of 0·7 of UTS, while in the case of maximum applied load of 0·75 of UTS the presented results are referred to the mean value of four specimens up to 100 kcycles, three specimens up to 140 kcycles and two specimens up to 170 kcycles. As it was expected all the tested samples, which are exposed to a maximum applied stress of 0·7 of UTS, were run out of the fatigue experiment (10^6 cycles), while in the case of maximum applied stress of 0·75 of UTS no specimen survived longer than 280 kcycles (mean fatigue life 174 kcycles and fatigue life for each testing sample 274, 101, 148 and 173 kcycles respectively). Figure 3 presents the variation of the normalised effective dynamic modulus of elasticity in the loading direction versus the fatigue cycles in both applied maximum stress levels. Solid symbols stand for maximum applied fatigue stress of 0·7 of UTS, while open symbols stand for maximum applied fatigue stress of 0·75 of UTS. According to these plots, there is a very steep but limited reduction of the effective dynamic modulus of elasticity, for both cases of loading, within the first 25 kcycles. This region and this behaviour mainly corresponds to the formation of matrix crack network and its extension up to the saturation point, the development of fibre–matrix debonding and the failure of some of the reinforcing fibres in the loading direction. These failure mechanisms are the reason for the monitored stiffness reduction.

Comparing the stiffness reduction caused in the two different maximum applied stress levels, it is clear that loading up to 0·75 of UTS produces higher decrease of effective dynamic modulus of elasticity, and this indicates additional fibre failures in this case (something which will be confirmed later based on the results of acoustic emission monitoring).

After the first 30 kcycles the effective dynamic modulus of elasticity remains almost constant, in case where the maximum applied load was 0·7 of UTS, while it keeps decreasing with a lower rate until the final fracture in case where the maximum applied load was 0·75 of UTS. It is very interesting to notice that the higher the frequency where the stiffness is calculated, the higher the effect of fatigue, and this is true for both cases of maximum loading.

However, in the case of 0·7 of UTS maximum applied load the highest monitored variation of the stiffness was 9% at the end of fatigue experiment, while when the maximum applied load was 0·75 of UTS then at the end of its life, the specimen appears a maximum stiffness decrease of 24%.

Figure 4 presents the variation of the normalised damping coefficient (loss factor), which corresponds to the monitored effective dynamic modulus of elasticity, versus the fatigue cycles for both applied maximum stress levels. Again the solid and the open symbols correspond to the different maximum applied stress level of 0·7 and 0·75 of UTS respectively.

As shown in Fig. 4 for both maximum applied stress levels and for all the three first eigenmodes, in each case the modal damping and the corresponding damping coefficient increases very fast within the first 25 kcycles. The rate of increase is almost the same for all the cases, although the monitored damping in the case of maximum applied load of 0·75 of UTS was higher for all the cases. After the 30 kcycles in the case of maximum applied load of 0·7 of UTS the damping coefficient keeps increasing, but at a lower rate. This rate remains almost constant until the end of the fatigue experiment. When the applied maximum fatigue load is 0·75 of UTS (exceeds the endurance

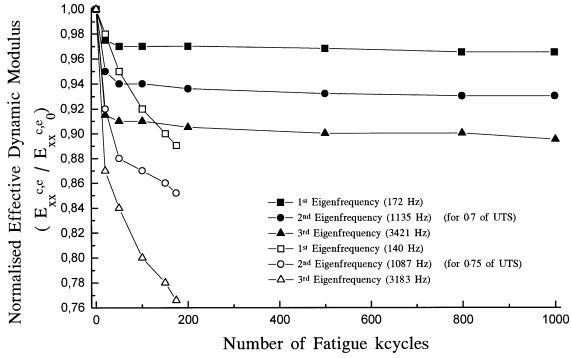

Fig. 3. Normalised effective dynamic modulus in the loading direction versus fatigue cycles of 3-D SiC/SiC for maximum applied stress of 0·7 (solid symbols) and 0·75 (open symbols) of UTS respectively.

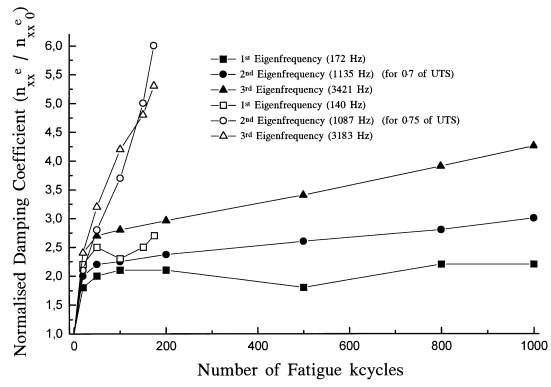

Fig. 4. Normalised damping coefficient (loss factor) versus fatigue cycles of 3-D SiC/SiC for maximum applied stress 0·7 (solid symbols) and 0·75 (open symbols) of UTS respectively.

fatigue limit) then the rate of increase of the material damping for all the first three eigenfrequencies remains high but slightly lower compared to the one appearing during the first stage, with the exception of the damping monitored for the first eigenfrequency.

After the threshold of 150 kcycles, all the surviving specimens appeared with a higher rate of increase for the material damping as they approach the end of their life. This was valid for all the eigenfrequencies. What it is very interesting to notice here is that the increase of damping during the first 25 kcycles is of the order of 170%, while the maximum damping increase for loading up to 0·7 of UTS was 320% and for loading up to 0·75 of UTS was 500%. Comparison of these values to the relative variation of effective dynamic modulus of elasticity, indicates that a loss factor or equivalently the damping of the relative eigenmodes is a much more sensitive parameter to fatigue damage compared to the effective modulus of elasticity. Furthermore, the fact that during the last stage of fatigue life (for maximum applied stress 0·75 of UTS), modal damping and the corresponding loss factor has a higher rate of increase. That could be easily explained by the development of fibre failures which will finally lead the fatigue sample to failure and could be used as an indicator to the stage of damage, forming a predictor for the on-coming material failure due to fatigue. The failure fibres create a new friction surface and establish new energy dissipation mechanisms, which are activated during the transverse vibration of the specimen and are monitored as damping increase.

Table 2 summarises the maximum normalised variations measured by using the dynamic response monitoring during the fatigue of 3-D SiC/SiC composites under two different maximum applied stress levels.

According to these results, in general, damping coefficient is a much more sensitive damage indicator compared to the effective dynamic modulus of elasticity and additionally the higher the eigenfrequency and the eigenmode used for the dynamic response monitoring of the material the more pronounced the measured variation is.

Table 2. Dynamic response monitoring of 3-D SiC/SiC of composites

$\sigma_{max}/\sigma_{ult}$	*Maximum applied fatigue cycles (kcycles)*	$(E_{xx}^{c,e}/E_{xx}^{c,e}{}_0)$ *min*	$(n_{xx}^{e}/n_{xx}^{e}{}_0)$ *max*
0·7	1000	f_1: 0·96	2·213
		f_2: 0·93	3·012
		f_3: 0·89	4·258
0·75	174	f_1: 0·89	2·716
		f_2: 0·85	5·342
		f_3: 0·77	6·084

3.2 Correlation with acoustic emission results

As has already been mentioned, during fatigue experiments at both maximum applied load levels, continuous AE monitoring was applied. Then, pattern recognition techniques were applied and the events which are related to fibre failure have been separated in order to be correlated to the stiffness degradation presented in the former Section. More precisely, the applied pattern recognition technique provides a new analysis algorithm of AE data and has been proposed elsewhere.[13] It contains descriptor selection procedures, validation steps, filtering and statistical analysis of AE data, taking into account the stochastic character of AE events and the failure mechanisms appearing in the specific material under consideration. A key point of the used algorithm is the cluster activation in time informing which increases the reliability of correlation between clusters and failure mechanisms. The corresponding results are given in Figs 5 and 6.

Both Figs 5 and 6 represent the AE events, which correspond to fibre breakage, as a function of the fatigue cycles for maximum applied stress of 0·7 and 0·75 respectively. The broken lines in both figures indicate the degradation of the normalised effective dynamic modulus versus fatigue cycles.

In general, these types of diagrams, have a bath-type shape that could be derived in three different regions[7]: (i) a Burn-in phase, (ii) a Steady–state region and (iii) a Burn-out stage. Regarding the Burn-in phase (in both Figures up to 25 kcycles), it accounts for fibre fracture events during the application of fatigue mean load and the first cycles of the fatigue test. The steady-state phase represents an increase of damage, which weakens the material structure, causing degradation of its performance

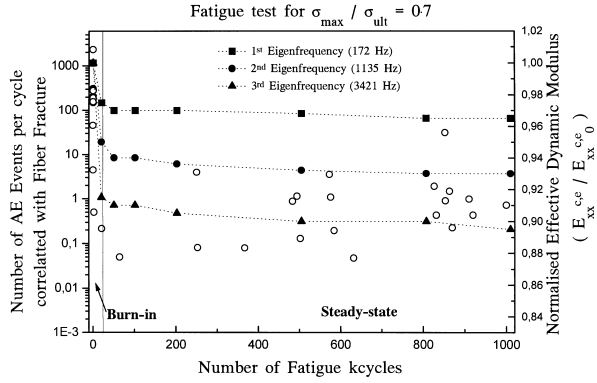

Fig. 5. Correlation between AE activity related to fibre fracture and normalised effective dynamic modulus for fatigue loading of 3-D SiC/SiC up to 0·7 of UTS.

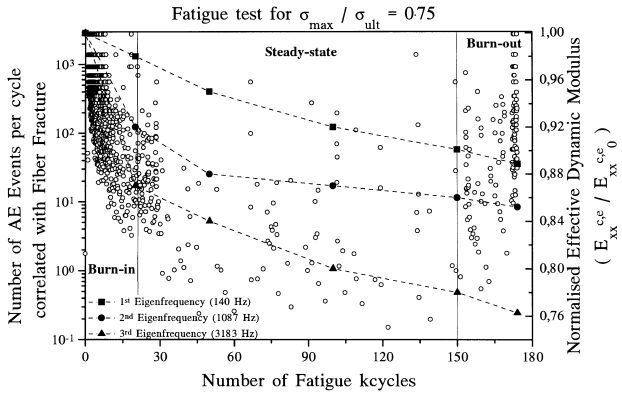

Fig. 6. Correlation between AE activity related to fibre fracture and normalised effective dynamic modulus for fatigue loading of 3-D SiC/SiC up to 0·75 of UTS.

and increase of internal damping. Due to the redistribution of the stress field around the fibre during this period, the crack saturation phase approaches and an unstable damage propagation initiates. This period involves an increase rate of fibre fracture and corresponds to the burn-out phase. It leads to the materials final failure. The burn out phase is absent from Fig. 5 since the material is loaded lower to its endurance fatigue limit. In contrast to this, in the case of Fig. 6 a more massive destruction of the material appears from the beginning of loading, since the applied load exceeds the endurance fatigue limit, the number of fibre breakages is higher and close to the end of the life of the material the burn out phase appears. These results are in good correlation with that provided by the monitoring of the dynamic response of the material during fatigue.

The monitoring of the dynamic response of the material could be accounted as a macroscopic approach, while the AE monitored stands for a microscopic approach and based on this, the critical role of fibre fracture on the 3-D SiC/SiC stiffness degradation could be confirmed. The degradation of the effective dynamic storage modulus is directly related to the number of fibre fractures and this is confirmed comparing the results presented in Figs 5 and 6. On the other hand, additionaly to the matrix cracking that occurred during fatigue loading, the failure of a fibre bundle leads to a stress redistribution in the vicinity of the broken fibre. This produces a stress concentration site, and as a result to fibre–matrix debonding. Then the friction is the only load transfer mechanism between matrix and fibres, but is the presence of this friction that is recognised as internal damping increase. Thus, the fibre fracture promotes fibre-matrix debonding and then friction plays a very critical role for the mechanical behaviour of CMCs during fatigue. The presence of the internal friction is monitored either through damping coefficient in our case or through the hysterisis loops elsewhere and could be a very reliable damage indicator for the material under investigation.

4 Conclusions

The present work deals with the characterisation of damage development in 3-D SiC/SiC composites under fatigue loading using as indicators of the fatigue damage the effective dynamic modulus of elasticity and the corresponding damping coefficient. The main conclusions of the present study are the following:

- The fatigue damage produces a progressive reduction of the effective dynamic modulus during the first 30 kcycles of fatigue life (for maximum applied stress of 0·7 of UTS) while the damping coefficient increases drastically.
- Damping coefficient is more sensitive to fatigue damage than the storage modulus.
- The damage stage associated to the interfacial wear and internal friction is very well correlated to the monitored damping coefficient
- The damping coefficient is in a direct relation to the elsewhere used area of the hysterisis loop[1] which is also a fatigue damage indicator in the case of CMCs.

The combination of dynamic response monitoring with other damage evaluation methods such as AE could be a powerful tool in the study of the fatigue damage of CMCs and could be used for establishing safe criteria for the stability of fatigue damage and the remaining life of the material under investigation.

Acknowledgements

The authors want gratefully to acknowledge the support of the Greek Ministry of Development, General Secretariat of Research and Technology to the present work within the frame of PENED project (Contract no. 615).

References

1. Evans, A. G., Zok, F. W. and McMeeking, R. M., Fatigue of ceramic matrix composites—overview. *Acta metall. Mater.*, 1995, **43**, 859–875.
2. Reynaud, P., Cyclic fatigue of ceramic-matrix composites at ambient and elevated temperatures. *Comp. Sci. and Tech.*, 1996, **56**, 809–814.
3. Evans, A. G., Design and life prediction issues for high-temperature engineering ceramics and their composites. *Acta Metall. Mater.*, 1997, **45**, 23–40.

4. Kotil, T., Holmes, W. J. and Comnimou, M., Origin of hysterisis during fatigue of ceramic-matrix composites. *J. Am. Ceram. Soc.*, 1990, **73**, 1879–1983.
5. Rouby, D. and Reynaud, P., Fatigue behaviour related to interface modification during load cycling in ceramic-matrix fibre composites. *Comp. Sci. and Tech.*, 1993, **48**, 109–118.
6. Holmes, J. W. and Sorensen, B. F., Fatigue behaviour of continuous fibre-reinforced ceramic mactrix composites. In *High Temperature Mechanical Behaviour of Ceramic Composites* eds. Nair, S. V. and Yakus, K., Butterworth-Heinemann, London, 1995, pp. 261–327.
7. Vellios, L., Pappas, Y. Z., Kostopoulos, V. and Paipetis, S. A., Fatigue damage characterization of 3-D SiC/SiC composites using non destructive techniques. In *High Technology Composites in Modern Applications*, eds. Paipetis, S. A. and Youtsos, A. G., AML/University of Patras, Patras, Greece, 1995, pp. 434–443
8. Kostopoulos, V., Vellios, L. and Pappas, Y. Z., Fatigue behavior of 3-D SiC/SiC composites. *J. Mat. Sc.*, 1997, **32**, 215–220.
9. Schoberth, A. W., Condlifel, I., Michorious, M., Kostopoulos, V., Martin, E. and Anifrani, J. C., Development and characterization of CMC and C/C composites, Publishable synthesis report of BRITE/EURAM Project, Contract N. BREU 0334-C, 1994.
10. Vellios, L., Kostopoulos, V. and Paipetis, S. A., Fatigue effect on dynamic characteristics of composite laminates. *Adv. Comp. Letters*, 1994, **5**, 121–128.
11. Vellios, L., Kostopoulos, V. and Paipetis, S. A., Fatigue damage growth monitoring of ud-composites using vibration and acoustic emission techniques. In *Proceedings of ICCM/9*, Vol. V, Composite Behaviour, ed. Miravete, A., University of Zaragoza, Woodhead Publishing Ltd., Zaragoza, Spain, 1993, pp. 811–818.
12. Physical Acoustic Corporation, 8000 SPARTAN AT Users Manual, PAC, NJ, USA, 1988.
13. Pappas, Y. Z., Markopoulos, Y. Z. and Kostopoulos, V., Failure mechanisms analysis of 2-D carbon/carbon using acoustic emission monitoring. *NDT&E Int.*, 1998, **31**, 157–163.
14. Korotzis, D. T., Vellios, L. and Kostopoulos, V., On the viscoelastic response of composite laminates (Viscoelastic Lamination Theory). *J. of Mech. of Time Dep. Mat.*, submitted.